On the Incorporation of Buckminsterfullerene C_{60} in the Supercages of Zeolite Y

German Sastre,[†] María Luz Cano,[†] Avelino Corma,*[,†] Hermenegildo García,[†] S. Nicolopoulos,[‡,§] J. M. González-Calbet,[‡,||] and M. Vallet-Regí[§,||]

Instituto de Tecnología Química CSIC-UPV, Universidad Politécnica de Valencia, Avenida Los Naranjos s/n, 46022 Valencia, Spain, Departamento de Química Inorgánica, Facultad de Químicas, Universidad Complutense, 2804 Madrid, Spain, Departamento de Química Inorgánica y Bioinorgánica, Facultad de Farmacia, Universidad Complutense, 28040 Madrid, Spain, and Instituto de Magnetismo Aplicado, RENFE-UCM, Apartado 155, 28230 Madrid, Spain

Received: November 21, 1996; In Final Form: September 4, 1997[⊗]

A series of vapor-phase adsorptions of C_{60} on NaY zeolite have been carried out under reduced pressure (1 Torr) in the range of temperatures between 400 and 700 °C to determine whether C_{60}-fullerene (0.79 nm diameter) can be incorporated within the internal voids of faujasites (tridirectional large-pore zeolite containing supercavities of 1.3 nm diameter tetrahedrally connected through 0.74 nm windows). After the incorporation procedure, the samples were submitted to exhaustive solid−liquid extraction using toluene as solvent. The optimum adsorption temperature was found to be around 650 °C. Analogous treatment using silica−alumina instead of NaY did not lead to significant retention of C_{60}. The samples were characterized by X-ray powder diffraction, combustion chemical analysis, and thermogravimetry-differential scanning calorimetry as well as by diffuse reflectance, Fourier transform infrared, and magic angle spinning ^{13}C NMR spectroscopies. None of these techniques provides direct evidence of the location of C_{60} in the zeolite matrix. Molecular dynamics simulations of the faujasite cavity window vibrations at different temperatures (100−800 °C) show that although there are remarkable instantaneous variations in the pore diameter (some of them allowing the entrance of fullerene molecules), the vibrations are too rapid (in the ps time scale) to allow the complete passage of fullerene. Interestingly, the average pore diameter of the faujasite cavity windows are predicted to be rather insensitive to increasing temperatures. Finally, high-resolution electron microscopy has experimentally revealed that fullerene molecules are highly dispersed through the zeolite particles, and in certain regions there are some preferential spatial arrangements of C_{60}. In addition, the presence of weak new reflections in the electron diffractogram pattern of C_{60}-doped NaY (forbidden for a *Fd*$\bar{3}$*m* symmetry such as Y zeolite) was observed. This has been taken as an experimental evidence that a small fraction of C_{60} molecules has penetrated inside the supercages, showing a spatial order and changing the zeolite symmetry. Meanwhile, most of the C_{60} molecules are located in the open cavities at the external surface.

Introduction

In order to gain control on the superconducting,[1,2] optical,[3−7] and other molecular properties[8−13] of buckminsterfullerene C_{60}, an intensive effort is being devoted to develop systems with a reduced dimensionality from tridimensional bulk material to supramolecular entities with zero-dimensionality with respect to the fullerene guest.[14−18] The last type of organized assemblies, commonly termed as quantum dots,[19−21] express the concept that in a particular situation each fullerene molecule would be isolated from the rest. In this way, intermolecular interactions could be simply avoided.

A general methodology to obtain isolated molecules consists of the confinement of a guest embedded within a rigid solid matrix, such as zeolites. Zeolites are microporous crystalline aluminosilicates, whose internal voids are accessible to organic guests when their molecular size is smaller than the aperture of the zeolite micropores.[22−24] In particular, taking into account that C_{60} is a spherical molecule of 7.9 Å of crystallographic diameter,[25−27] previous studies have been directed to incorporate C_{60} within extra large pore aluminophosphates such as VPI-5, $AlPO_4$-5, and $AlPO_4$-8, where the channel dimension is in all cases higher than the crystallographic diameter of C_{60}.[28,29] However, this strategy is flawed by the extreme lability of these hosts compared to robust classical zeolites and by the fact that, once inside the channels, there is not a physical barrier to immobilize C_{60} within the pores. In addition, since the topology of these AlPOs is formed by a unidirectional array of channels, only one-dimensional lines and no zero-dimensional dots can be obtained.

The use of AlPOs has been justified by the physical impossibility to adsorb C_{60} within conventional large-pore zeolites, such as faujasites, whose pore apertures are typically 7.4 Å.[30] However, it has to be remarked that the window opening of faujasites supercages are smaller, but not much different than the diameter of undisturbed C_{60} (7.9 Å). Therefore, the simple acceptance of these crystallographic values to rule out the absorption of C_{60} in faujasites may be misleading, since a more rigorous approach must consider the kinetic diameters of the host apertures resulting from the vibrations of the lattice at different temperatures as well as the energy barrier required to deform the guest allowing it to cross the window openings. No such methodology has been applied to predict the possibility of incorporation of C_{60} in faujasites. Worth noting is that even the simplest molecular modeling indicates that fullerenes can be easily accommodated within the faujasite supercages which are almost spherical cavities of 13 Å of diameter interconnected tetrahedrally to four neighbor super-

[†] Universidad Politécnica de Valencia.
[‡] Facultad de Químicas, Universidad Complutense.
[§] Facultad de Farmacia, Universidad Complutense.
[||] RENFE-UCM.
[⊗] Abstract published in *Advance ACS Abstracts,* November 15, 1997.

S1089-5647(96)03883-7 CCC: $14.00

cages, through windows of 2.5 Å depth. The topology of the supramolecular assembly resulting after the encapsulation of C_{60} within the faujasite cages indicates that only one molecule could fit in each cavity and the framework would be insulating each molecule avoiding or diminishing the interaction with the neighbors in next nearest cages.

In the present work, we have carried out the incorporation of C_{60} from the vapor phase within the Na^+ form of Y faujasite at high temperatures. As both C_{60} and faujasite exhibit a remarkable thermal stability in the absence of any reagent, it is possible to heat this system well above 1000 K under inert atmosphere without destroying the crystalline structure of the faujasite or decomposing C_{60}. These conditions are essentially different to those that have attempted the incorporation of C_{60} in the liquid phase or at relatively mild temperatures, since the kinetic energy of the guest and the vibrations of the lattice would dominate the diffusion phenomena. Molecular dynamics simulations of the faujasite cavity window vibrations at different temperatures (100−800 °C) show that lattice vibrations are too rapid (in the ps time scale) to allow the complete passage of fullerene. Finally, we have carried out a high-resolution electron microscopy study of the resulting samples providing evidence that only a very small fraction of C_{60} has penetrated, at least partially, inside the solid crystallites while most of the fullerene molecules are located in the open cavities at the external surface.

Results and Discussion

Recent reports have described the adsorption of C_{60} in faujasite-type zeolites assuming the internal location of fullerene molecules without providing direct experimental evidence supporting the incorporation inside the pores.[31−36] These reports appear to be contradictory with the need of employing extra large pore zeotypes claimed by different authors.[28,29]

In our case, adsorption was carried out by heating progressively under reduced pressure (1 Torr) a mechanical mixture of C_{60} and hydrated NaY (Si/Al = 2.4) up to the corresponding temperature that was maintained for 1 h. The range of final temperatures studied was between 400 and 750 °C. After the vapor-phase adsorptions, the samples were submitted to continuous solid−liquid extractions using toluene as solvent. It is known that C_{60} is poorly soluble in the majority of organic solvents, being slightly soluble in benzene and toluene. The sample was periodically outgassed and checked by X-ray diffraction. The extraction procedure was continued for extended periods until the more intense peaks in the diffractogram of pure C_{60} at $2\theta = 10$, 17, and 21° could not be detected. Absence of the characteristic C_{60} peaks in the diffraction pattern of the powders has been previously considered as a proof of the inclusion of fullerene in the micropores of the particles. However, this piece of evidence does not rigorously rule out the possibility that fullerene molecules would be highly dispersed, but exclusively on the external surface of the zeolite particles. Thus, it is reasonable to assume that, during the sublimation at high temperatures, the crystals of C_{60} have collapsed and the C_{60} molecules are deposited on the external and/or internal surfaces of the zeolite. There is no guarantee that the diffusion through the micropores has occurred.

Liquid-phase adsorptions of thermally dehydrated NaY that was mixed with solutions of C_{60} in toluene at 110 °C for 3 h lead after extraction to white solids, indicating that fullerene incorporation did not take place. Likewise, white solids were obtained after vapor-phase adsorptions at temperatures below 550 °C or above 700 °C. The optimum temperature for the vapor incorporation under our experimental conditions was found to be about 650 °C. Samples prepared in this way

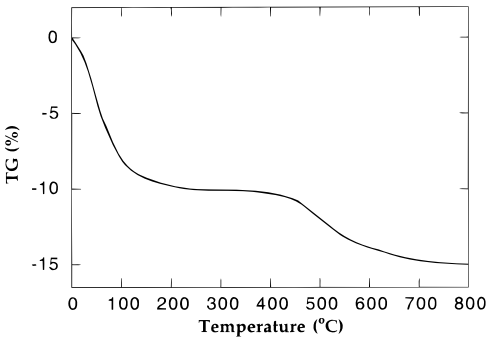

Figure 1. Termogravimetry (TG %) of C_{60}−NaY sample prepared by vapor-phase adsorption at 600 °C.

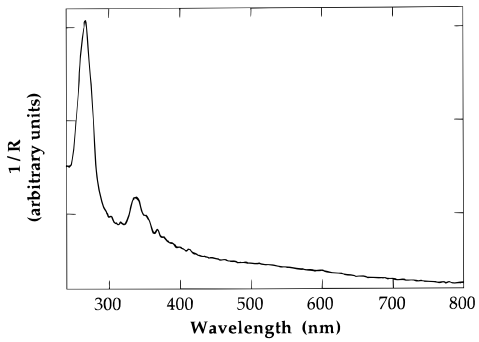

Figure 2. Diffuse reflectance spectrum (as inverse of the reflectivity, 1/*R*) of the C_{60}-doped NaY after solid−liquid extraction.

remained black after exhaustive solid−liquid extraction, although some C_{60} could be partially recovered during the extraction with toluene. We believe that if the temperature is below 550 °C, the sublimation is not very efficient, while for temperatures above 700 °C the vapor partial pressure is too high and C_{60} is finally pumped out of our system.

Interestingly, we performed a control experiment working at 650 °C using amorphous silica−alumina instead of zeolite. The objective was to determine if our extraction procedure is efficient to recover all C_{60} from nonmicroporous solids such as silica−alumina. As a matter of fact, the resulting solid after vapor adsorption and toluene extraction was white, and no C_{60} was detected by diffuse reflectance spectroscopy. This control points out the importance of the host microporosity in the adsorption of C_{60}. Even if C_{60} molecules were dispersed exclusively at the exterior of the faujasite crystals, these surfaces are not flat, but formed by the pore openings and partial, uncompleted cavities that will hold the spherical molecules of fullerenes like eggs in nests.

The samples were carefully outgassed under reduced pressure (10^{-2} Torr) to ensure total evacuation of residual toluene and then submitted to an array of characterization techniques. Carbon combustion chemical analysis established that the loading level was 32 mg of C_{60} per gram of solid (4.4×10^{-2} mmol g^{-1}). This loading would correspond to ca. one monolayer of the fullerene on the zeolite (19 m^2 g^{-1} external surface area). Thermogravimetry coupled with differential scanning calorimetry (TG-DSC) profiles provide a useful information about the homogeneity of the samples and desorption temperatures. High desorption temperatures have been previously considered as indicative of the incorporation of C_{60} into the channels of VPI-5. Figure 1 shows the TG-DSC of our C_{60}−HY samples prepared by vapor-phase adsorption at 600 °C. As it can be seen, there is an initial loss of weight at temperatures below 150 °C that can be ascribed to desorption of coadsorbed water. The subsequent loss of weight was smooth and agrees well with the total carbon content as determined by

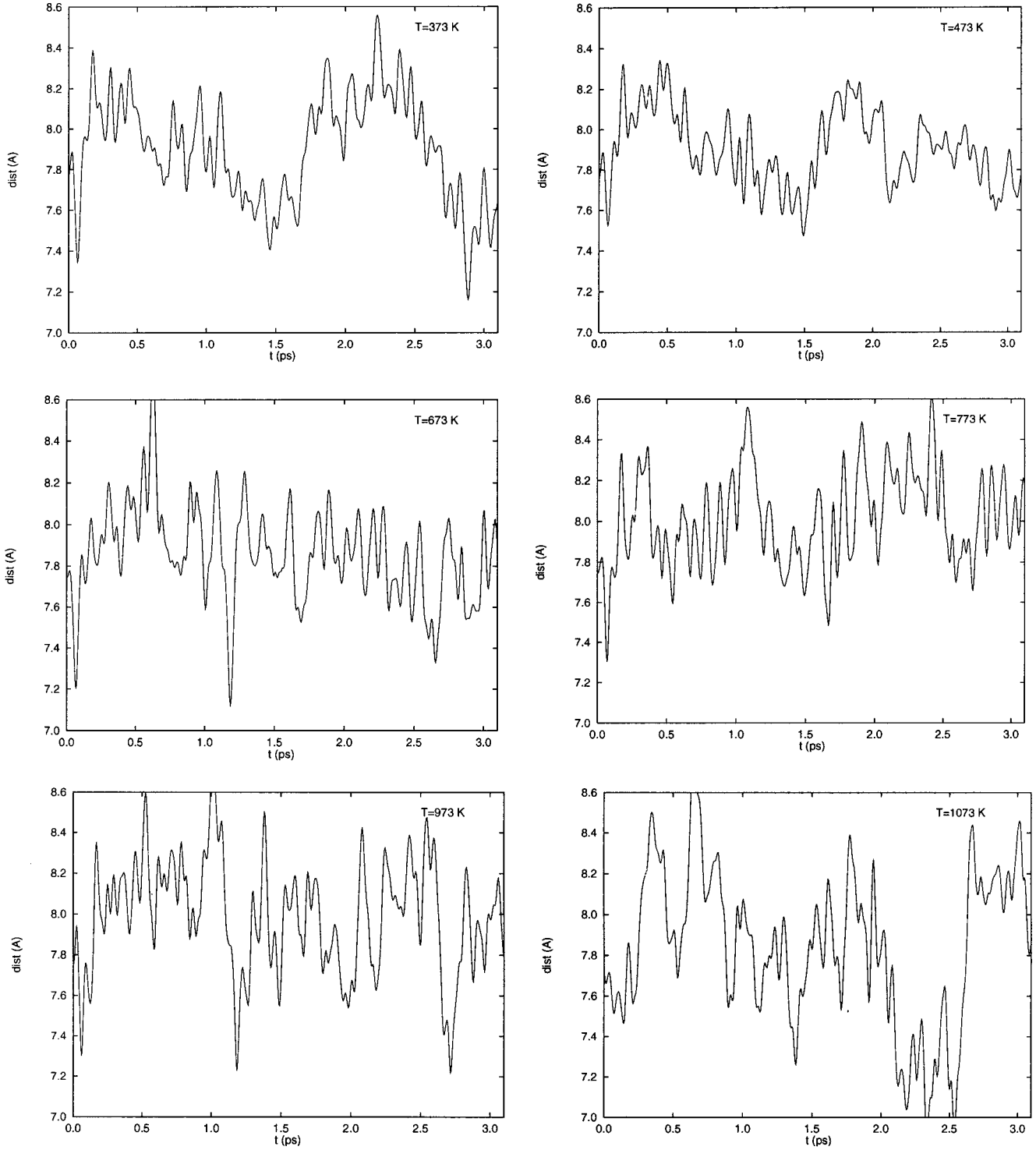

Figure 3. Results of the molecular dynamic simulation on the all-silica faujasite cavity window at $T = 373$, 473, 673, 773, 973, and 1073 K. The selected distances (in Å) correspond to 12MR diameters of one of the supercavity window openings.

combustion analysis. The corresponding DSC curve shows a broad exothermic process from 400 to 600 °C, peaking at 530 °C. Since TG-DSC profiles were obtained under air stream, this exothermic peak would correspond to the partial oxidation/degradation of C_{60}. The broadness of the peak may suggest that adsorbed C_{60} is widely distributed in different environments on the zeolite particles. Noticeably, the reported desorption temperatures for other microporous materials are much higher than the mean value measured here. However, taking into account the low loading levels, the low sensitivity of this technique and the presumably heterogeneous distribution of the guest, this does not rule out that a portion of C_{60} may be encaged in the interior of the particle.

Diffuse reflectance spectra of the black C_{60}−NaY could be recorded after blending the nonreflecting samples with additional amounts of NaY (Figure 2). The spectra showed the characteristic absorption bands corresponding to C_{60} in hexane solution.[37,38] On the other hand, concerning IR spectroscopy, it is known that C_{60} does not have intense vibration bands owing to its remarkable symmetry.[39,40] In previous related work about the incorporation of C_{60} in $AlPO_4$-8, three of the four IR bands of C_{60} could not be detected because they were superimposed

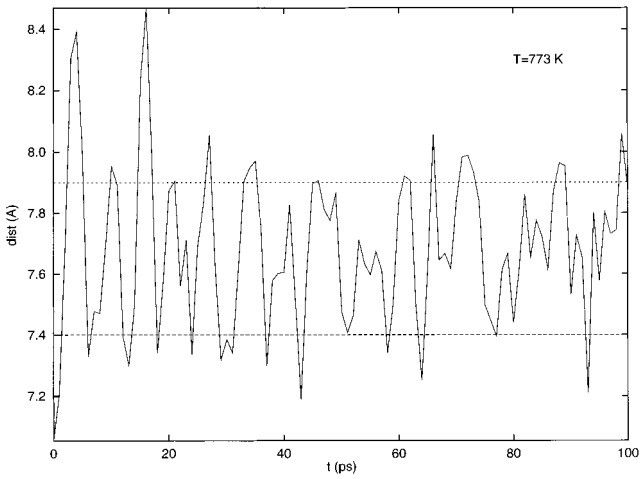

Figure 4. Long time simulation run ($T = 673$ K) showing the faujasite 12MR window diameter, the faujasite crystallographic diameter, and the C_{60} diameter.

on the intense vibration bands of the $AlPO_4$-8 lattice, and only at high loading (0.5 g of C_{60} per gram of $AlPO_4$-8) was the band at 1430 cm^{-1} detectable over the spectrum background. In our case, owing to the much lower loading level (0.032 g of C_{60} per gram of NaY), we were not able to observe any of the four IR bands of C_{60} because they are probably very weak compared to the absorption of the framework aluminosilicate bands. Worth noting was the fact that no absorptions owing to residual toluene from the solid−liquid extraction procedure were detected either, thus providing the useful information that the evacuation of this solvent was carried out efficiently.

Solid-state magic angle spinning (MAS) ^{13}C NMR of our samples were also recorded. A single peak at 144.2 ppm was observed. This chemical shift is very similar to that previously reported for pure C_{60} in solid state.[39,41−43] However, two different chemical shifts (151 and 145.6 ppm) have been reported for C_{60} incorporated within VPI-5. In any case, the lack of variation of the chemical shift of C_{60} adsorbed on NaY compared to its crystals does not rigorously indicate the internal or external location of fullerene molecules in the zeolite particles. In fact, it would be more reasonable to expect C_{60} to be widely distributed within different environments of the zeolite framework, and a single ^{13}C NMR peak does not provide much information in this sense. A more conclusive piece of evidence is needed in order to assess this point. Therefore, we think that none of the above characterization techniques provides a direct information of the location of C_{60} through the zeolite network. Before commenting on the high-resolution electron microscopy of C_{60}−NaY samples, theoretical calculations were undertaken to gain understanding on the diffusion phenomenon of C_{60} through the faujasite lattice.

Simulation of Diffusion of C_{60} through Faujasite Supercages. Molecular dynamics calculations have been performed to simulate the vibrations and pore fluctuation of Y zeolite at different temperatures. The Discover 3.1[44] code was used for these simulations in which an all silica Y zeolite was employed for simplicity and also to concentrate our efforts not in studying the cation distribution with the temperature but only the framework relaxation. The cvff potential[45] was considered in the simulations, that potential being described as a sum of electrostatic and covalent terms, the latter corresponding to a Buckingham potential for the interaction between two atoms, a three-body term to consider O−Si−O interactions, and different terms to quantify the interactions involving more than three atoms. This kind of approach has been successfully used in modeling structure and characterization of zeolites.[46,47] In

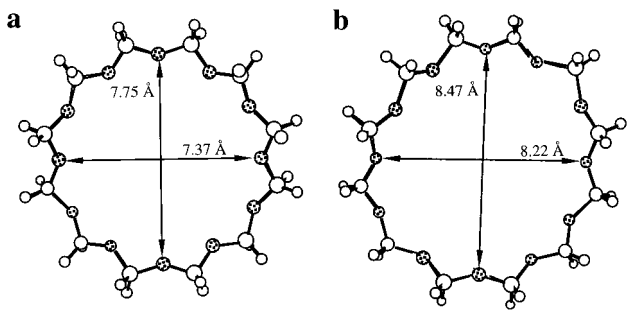

Figure 5. Diameters (vertical and horizontal) of the 12MR faujasite window. (a) crystallographic, (b) configuration selected after molecular dynamics simulation at $T = 673$ K.

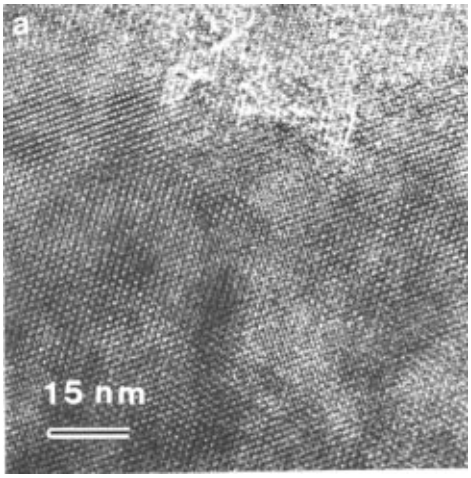

Figure 6. HREM micrograph recorded along the [110] axis of a Y particle doped with C_{60}.

particular, dynamic pore openings in zeolites have also been studied recently with this methodology.[48,49] Although the flexibility of the T−O−T bonds is one of the most peculiar features zeolites,[50−54] not all the zeolites have the same flexibility, and thus, there is no general orientation about what the change in the pore size is after vibrational effects are considered. Our molecular dynamics study was carried out applying periodic boundary conditions, thus modeling a unit cell of purely siliceous Y zeolite and taking into account its periodicity. This is an essential condition of our simulation if vibrational properties are to be extracted from the results. The NPT (constant number of particles, pressure, and temperature) ensemble was considered throughout the simulations, and atmospheric pressure was selected in all the calculations. The set of temperatures chosen were 373, 473, 673, 773, 973, and 1073 K. A first initialization stage of 0.1 ps, was run to ensure that the energy was constant, and the simulation was then extended for another 3.0 ps. The time step used was 0.001 ps, and history files were saved every 0.01 ps. The Verlet[55] integration algorithm was used in the simulations. The results obtained at the different temperatures (Figure 3) show that there are important fluctuations in the 12 MR window of the faujasite structure. To confirm whether the models presented in Figure 3 describe correctly the vibrational motion of the Y framework, the simulation at 673 K was extended until 100 ps. The final plot (Figure 4) shows a pattern very similar to the results obtained in the previous shorter simulations (Figure 3). We also can notice from Figure 3 that the pore opening cannot be considered to increase or decrease with the temperature. Some of the plots seem to indicate slightly wider averages than others but no correlation with temperature has been found from our results. Nevertheless, it can be clearly observed that the Y pore dimension after the simulations differs from the crystallographic

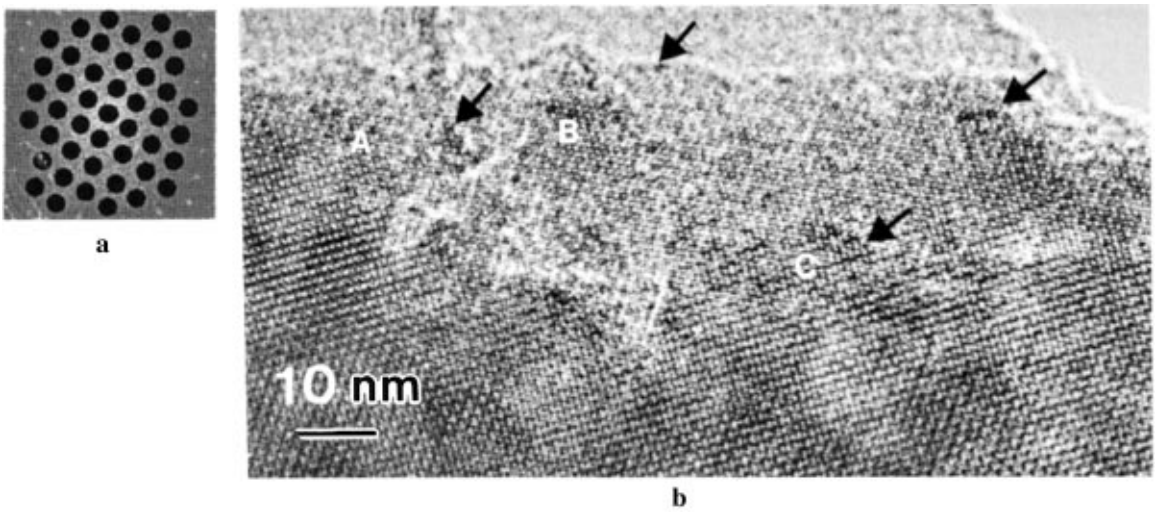

Figure 7. Fourier transformed diffractogram (a) and its corresponding enlarged processed HREM image (b) showing improved contrast of the highly dispersed fullerene molecules. Contrast for individual fullerene molecules have been marked with arrows.

value, 7.4 Å.[56] The results shown in Figure 4 indicate that some of the instantaneous values of the window dimensions would allow the entrance of the C_{60} molecule through the pore (Figure 5) whose opening has enlarged its diameter around 1.0 Å. We have considered the C_{60} as difficult to be deformed, since the single NMR peak suggests that it is rigid. Although Figure 5b shows one of the largest conformations for the 12MR during the dynamic simulation at 673 K, the plots in Figures 3 and 4 show that the pore window remains in that conformation a very short period of time, as the rapid oscillations in the diagrams show (Figures 3 and 4). Framework oscillations are therefore too rapid to allow the diffusion of C_{60} into the faujasite 12MR pore.

Electron Microscopy Study of the C_{60}−NaY Sample. Besides the previous simulation, direct information about the local structural distribution on an atomic scale can only be obtained by high-resolution electron microscopy (HREM) together with electron diffraction studies.[57−60]

The crystalline structure of faujasite consists of the three-directional cubic arrangement of large supercages (13 Å diameter) connected by twelve MR windows (7.4 Å diameter) and constructed from sodalite cages linked via D6R to four other sodalite cages. The space group is $Fd\bar{3}m$ with the lattice parameter $a = 24.7$ Å. According to previous HREM studies, the 12MR apertures are best observed along the [110] direction. Figure 6 shows such [110] image for a C_{60}-doped NaY zeolite prepared by vapor-phase adsorption at 600 °C. The large white dots in the HREM image correspond to the apertures of the supercages.

The strong contribution of the framework in the direct HREM image masks the contrast from fullerene molecules. This is commonly observed in HREM when the electrons are incident parallel to the directions of the pore opening. To circumvent this problem three general techniques have been devised: HREM of serial ultrathin sectioned specimens,[61] the *Z*-contrast method,[62] and image processing.[58,59] Herein we have used image-processing techniques and provide experimental evidence that the zeolite lattice imposes a preferential arrangement of some C_{60} molecules, indicating that some C_{60} are hosted in the zeolite structure.

The image of Figure 6 was digitized by scanning and then was Fourier transformed to obtain a diffractogram (Figure 7a). By placing small windows around all fundamental spots (including the [000] contribution which contains only non-periodic information), a subsequent inverse Fourier transformation strongly suppressed high-frequency nonperiodic noise from the image (Figure 7b). The filtered image clearly shows regions of randomly distributed dark contrast. Such abrupt changes in the contrast seem not to be related with local thickness changes.

Usually, molecules are detected from the shape and darkness of the contrast of the matrix structure.[59,60,63] The shape and darkness of the contrast in Figure 7b presumably indicates the presence of randomly dispersed fullerene particles into the structure. Moreover, in some areas of the same crystal, contrast of isolated individual molecules of approximate 10 Å in size can be seen (see arrows in Figure 7b), some of them lying on the surfaces of the crystal.

To better visualize the location of the fullerene particles in relation to the zeolite matrix, we processed three different regions of the HREM filtered image (labeled as A, B, and C in Figure 7b). The distinct image contrast of these regions probably reflect different fullerene repartition in relation to the zeolite structure. Image processing of these three regions was performed as before by placing small windows around all fundamental spots in the corresponding digital diffractograms and performing an inverse Fourier transformation. All diffractograms show information up to a resolution of 0.3 nm. The processed images are presented in Figure 8 a−c.

Processed images (Figure 8) clearly show that the dark contrast—presumably related with presence of fullerene particles—is not uniformly distributed throughout the zeolite matrix, and a preferential aggregation of the particles can be observed along (111) and (110) type planes through the Y crystal (see arrows). Nevertheless it is not possible to state if fullerenes stay on the surface (preferentially along certain directions) or if they are (at least partially) incorporated into the structure.

To address this point we have undertaken a careful study of the diffraction pattern of C_{60}-doped NaY zeolites. In these diffractions we observed weak [hhl] reflections with *h,l* not having the same parity (see arrows in Figure 9). Those reflections are forbidden for the $Fd\bar{3}m$ space group. This finding could suggest that a number of molecules have been incorporated into the crystalline structure producing an artificial lattice of fullerenes confined within the Y supercages which results in the new symmetry observed in diffraction. The weakness of these reflections would suggest that only a small amount of C_{60} has been encapsulated inside the zeolite lattice. However, such changes in symmetry (reflections forbidden for the $Fd\bar{3}m$ group) could also be an artifact induced by heat transformation under electron irradiation.

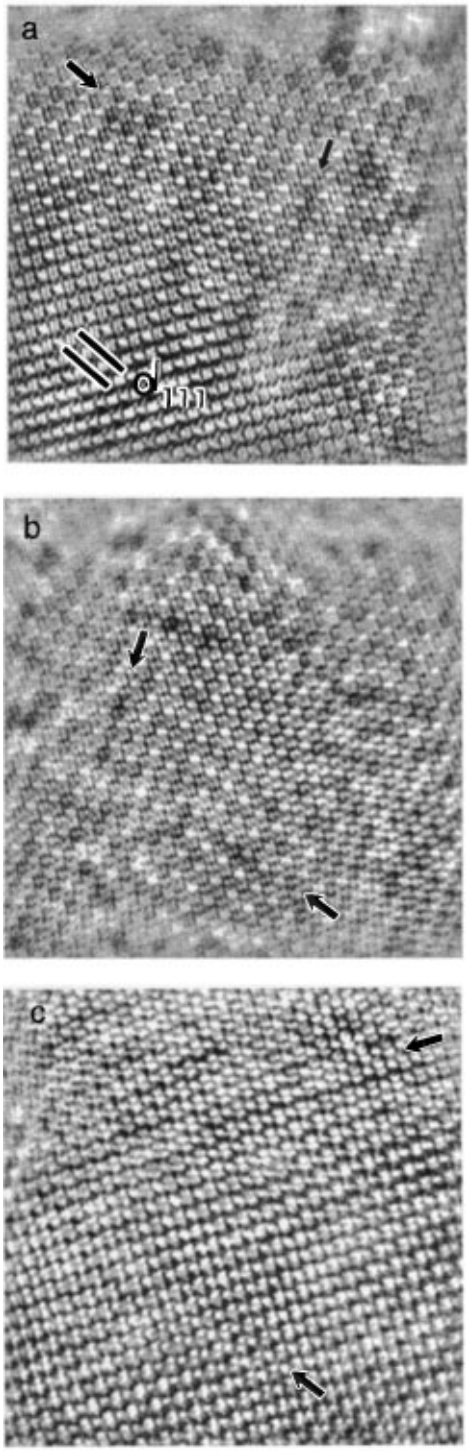

Figure 8. Expanded filtered HREM images (a,b,c) corresponding to the A, B, C region of the image of Figure 7.

In order to rule out this possibility, we performed HREM and diffraction experiments on a blank zeolite (not doped).

As anticipated, owing to the absence of any guest and the robustness and stability of the zeolite structure, no contrast due to partial destruction of the zeolite framework is observed; on the other hand, on the diffraction pattern (Figure 9) no extra spots have been detected (like the weak ones observed in Figure 7). The latter results further support the evidence that a certain incorporation of C_{60} into the Y structure has occurred.

Conclusions

HREM has shown that after vapor-phase adsorption of C_{60} on NaY zeolite, the fullerene molecules are highly dispersed on the solid particle although the distribution is not completely uniform. The spatial arrangement observed for some of the guest molecules indicates that they are hosted in the crystalline lattice either in the pore openings and partial cavities of the external surface or inside the cavities. The diffraction pattern of the C_{60}-doped NaY proves that, unlike what has been claimed in some previous reports, only very little of the fullerene has penetrated into the cavities, and most of it is located in the open cavities at the external surface. These experimental observations completely agree with the theoretical simulations that predict a highly impeded diffusion of fullerene molecules through the cavity windows of faujasite.

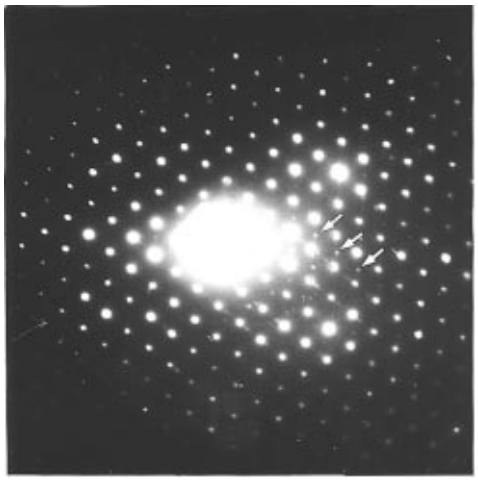

Figure 9. Electron diffraction pattern of C_{60}−NaY along the [110] axis. The weak lattice reflections marked with arrows are forbidden for the $Fd\bar{3}m$ symmetry group of Y faujasite.

None of the conventional characterization techniques previously used in the literature to study C_{60}-doped zeolites such as thermogravimetry-differential scanning calorimetry, IR or solid state ^{13}C NMR, and powder X-ray diffraction have been found to be appropriate to address the location of the guest.

Experimental Section

C_{60}-fullerene (Aldrich), NaY (Union Carbide SK-40), and silica−alumina (25% of Al_2O_2, BASF) were commercial samples and were used as received. Adsorptions of C_{60} were carried out by heating a mechanical mixture of C_{60} (40 mg) and NaY zeolite (500 mg) in an oven under reduced pressure (1 Torr) for 1 h. The samples were thoroughly extracted in micro Soxhlet equipment using CH_2Cl_2 as solvent. Periodic X-ray diffraction controls of the solid were undertaken up to the diffraction bands of pure C_{60} at $2\theta = 10$, 17 and 21° and were not detected. Combustion chemical analyses were performed in a Perkin-Elmer analyzer. Thermogravimetry-differential scanning calorimetry test were carried out in a Netsch STA 409 EP thermobalance under air stream using kaolin as standard. The heating rate was 10 °C min^{-1}. Diffuse reflectance spectra were recorded in a Shimadzu UV-2101 PC spectrophotometer using an integration sphere after mixing the black nonreflecting powder with additional amounts of white NaY. Fourier transform infrared spectroscopy of the C_{60}−NaY were recorded at room temperature in a greaseless quartz cell fitted with CaF_2 windows using a Nicolet spectrophotometer connected to a work station. Wafers of self-consistent zeolites samples (10 mg) were obtained by pressing the powder at 4 ton cm^{-2}. Solid-State MAS ^{13}C NMR of C_{60}−NaY were obtained using a Varian Unity +. Specimens of C_{60}-doped NaY for HREM were crushed in an agate mortar under acetone, then collected in a microgrid, and examined in a JEOL 4000EX high-

resolution electron microscope fitted with a top-entry goniometer and operated at 400 kV. HREM images were processed with CRISP software running on a personal computer.[64,65] The micrographs were scanned with an EPSON GT9000 scanner and then transferred to a 486/50 MHz PC Compaq.

Acknowledgment. Financial support by the Spanish DGICYT (Grant no. PB93-380) and partial funding by the European Commision within the Human Capital and Mobility program (CHR-CT93-0280) is gratefully acknowledged. M.L.C. also thanks the Spanish Ministry of Education for a postgraduate scholarship. We thank Prof. V. Fornés and Dr. W. Kolodziejski for the recording of FT-IR and MAS ^{13}C NMR spectra of the samples.

References and Notes

(1) Haddon, R. C.; Hebard, A. F.; Rosseinsky, M. J.; Murphy, D. W.; Duclos, S. J.; Lyons, K. B.; Miller, B.; Rosamilia, J. M.; Fleming, R. M.; Kortan, A. R.; Glarum, S. H.; Makhija, A. V.; Muller, A. J.; Eick, R. H.; Zahurak, S. M.; Tycko, R.; Dabbagh, G.; Thiel, F. A. *Nature* **1991**, *350*, 320−322.

(2) Glarum, S. H.; Duclos, S. J.; Haddon, R. C. *J. Am. Chem. Soc.* **1992**, *114*, 1993−2001.

(3) Abe, S.; Shimoi, Y.; Shakin, V. A.; Harigaya, K. *Mol. Cryst. Liq. Cryst. A*, **1994**, *256*, 97−104.

(4) Benner, R. E.; Dick, D.; Wei, X.; Jeglinski, S.; Vardeny, Z. V.; Moses, D.; Srdanov, V. I.; Wudl, F. *Mol. Cryst. Liq. Cryst. A.* **1994**, *256*, 241−250.

(5) Bunker, C. E.; Lawson, G. E.; Sun, Y. P. *Macromolecules* **1995**, *28*, 3744−3746.

(6) Khoo, I. C. *Opt. Lett.* **1995**, *20*, 2137−2139.

(7) Yoshino, K.; Akashi, T.; Yoshimoto, K.; Yoshida, M.; Morita, S.; Zakhidov, A. A. *Mol. Cryst. Liq. Cryst. A* **1994**, *256*, 343−357.

(8) Anpo, M.; Zhang, S. G.; Okamoto, S.; Yamashita, H.; Gu, Z. *Res Chem. Int.* **1995**, *21*, 631−642.

(9) Dai, S.; Sigman, M. E.; Burch, E. L., *Chem. Mater.* **1995**, *7*, 2054−2057.

(10) Delmonte, F.; Levy, D. *Chem. Mater.* **1995**, *7*, 292−298.

(11) Dresselhaus, M. S.; Dresselhaus, G. *Annu. Rev. Mater. Sci.* **1995**, *25*, 487−523.

(12) Lane, P. A.; Shinar, J. *Phys. Rev. B* **1995**, *51*, 10028−10038.

(13) Yoshino, K.; Yin, X. H.; Akashi, T.; Yoshimo, K.; Morita, S.; Zakhidov, A. A. *Mol. Cryst. Liq. Cryst. A* **1994**, *225*, 197−211.

(14) Maggini, M.; Scorrano, G.; Prato, M.; Brusatin, G.; Innocenzi, P.; Guglielmi, M.; Renier, A.; Signorini, R.; Meneghetti, M.; Bozio, R. *Adv. Mater.* **1995**, *7*, 404−406.

(15) Gvishi, R.; Bhawalkar, J. D.; Kumar, N. D.; Ruland, G.; Narang, U.; Prasad, P. N.; Reinhardt, B. A. *Chem. Mater.* **1995**, *7*, 2199−2202.

(16) Zhu, L.; Li, Y. F.; Wang, J.; Shen, J. *J. Appl. Phys.* **1995**, *77*, 2801−2803.

(17) Zhu, L.; Li, Y. F.; Wang, J.; Shen, J. *J. Chem. Phys. Lett.* **1995**, *239*, 393−398.

(18) Williams, R. M.; Zwier, J. M.; Verhoeven, J. W. *J. Am. Chem. Soc.* **1994**, *116*, 6965−6966.

(19) Zhu, K. D.; Gu, S. W. *Commun. Theor. Phys.* **1993**, *20*, 421−426.

(20) Geyler, V. A.; Popov, I. Y. *Zeitsch. Phys. Sect. B* **1994**, *93*, 437−439.

(21) Liu, A. S. *Phys. Rev. B* **1994**, *50*, 8569−8576.

(22) Breck, D. W. *Zeolite Molecular Sieves: Structure, Chemistry and Use;* John Wiley and Sons: New York, 1974.

(23) Barrer, R. M. *Zeolites and Clay Minerals as Sorbents and Molecular Sieves;* Academic Press: London, 1978.

(24) *Introduction to Zeolite Science and Practice;* van Bekkum, H.; Flanigen, E. M.; Jansen, J. C., De.; Elsevier: Amsterdam, 1991.

(25) Hawkins, J. M.; Meyer, A.; Lewis, T. A.; Loren, S.; Hollander, F. J. *Nature* **1991**, *252*, 312−313.

(26) Crane, J. D.; Hitchcock, P. B.; Kroto, H. W.; Taylor, R.; Walton, D. R. M. *J. Chem. Soc., Chem. Commun.* **1992**, 1764−1765.

(27) Hawkins, J. M. *Acc. Chem. Res.* **1992**, *25*, 150−156.

(28) Gügel, A.; Müllen, K.; Reichert, H.; Schmidt, W.; Schön, G.; Schüth, F.; Spickermann, J.; Titman, J.; Unger, K. *Angew. Chem., Int. Ed. Engl.* **1993**, *32*, 556−557.

(29) Anderson, M. W.; Shi, J.; Leigh, D. A.; Moody, A. E.; Wade, F. A.; Hamilton, B.; Carr, S. W. *J. Chem. Soc., Chem. Commun.* **1993**, 553−536.

(30) Meier, W. M.; Olson, D. H. *Atlas of Zeolite Structure Types;* Butterworth: London, 1992.

(31) Slinkin, A. A.; Emberson, S. C.; Derouane, E. G., *Kinet. Catal.* **1994**, *35*, 102−105

(32) Keizer, P. N.; Morton, J. R.; Preston, K. F.; Sugden, A. K. *J. Phys. Chem.* **1991**, *95*, 7117−7118.

(33) Anpo, M.; Zhang, S. G.; Okamoto, S.; Yamashita, H.; Gu, Z. *Res. Chem. Interm.* **1995**, *21*, 631−642.

(34) Gu, G.; Ding. W. P.; Cheng, G. X.; Zang, W. C.; Zen, H.; Du, Y. W. *Appl. Phys. Lett.* **1995**, *67*, 326−328.

(35) Gu, G.; Ding W. P.; Cheng, G. X.; Zang, W. C.; Zen, H.; Zhan, J. R.; Du, Y. W. *Modern Phys. Lett. B* **1995**, *9*, 1327−1332.

(36) Hutchings, G. J.; Cairns, I. T.; Saberi, S. P. *Catal. Lett.* **1995**, *30*, 131−134.

(37) Ajie, H.; Alvarez, M. M.; Anz, S., J.; Beck, R. D.; Diederich, F.; Fostiropoulos, K.; Huffman, D. R.; Krätschmer, W.; Rubin, Y.; Schriver, K. E.; Sensharma, K.; Whetten, R. L. *J. Phys. Chem.* **1990**, *94*, 8630−8633.

(38) Catalán, J.; Elguero, J. *J. Am. Chem. Soc.* **1993**, *115*, 9249−9252.

(39) Cox, D. M.; Behal, S.; Disko, M.; Gorun, S. M.; Greaney, M.; Hsu, C. S.; Kollin, E. B.; Millar, J.; Robbins, J.; Robbins, W.; Sherwood, R. D.; Tindall, P. *J. Am. Chem. Soc.* **1991**, *113*, 2940−2944.

(40) Hare, J. P.; Dennis, T. J.; Kroto, H. W.; Taylor, R.; Allf, A. W.; Balm, S.; Walton, D. R. M. *J. Chem. Soc. Chem. Commun.* **1991**, 421−413.

(41) Taylor, R.; Hare, J. P.; Abdul-Sada, A.; Kroto, H. W. *J. Chem. Soc., Chem. Commun.* **1990**, 1423−1425.

(42) Yannoni, C. S.; Johnson, R. D.; Meijer, G.; Bethume, D. S.; Salem, J. R. *J. Phys. Chem.* **1991**, *95*, 9−10.

(43) Tycko, R.; Haddon, R. C.; Dabbagh, G.; Glarum, S. H.; Douglas, D. C.; Mujsce, A. M. *J. Phys. Chem.* **1991**, *95*, 518−520.

(44) *Discover, Version 3.1*; Molecular Simulations/Biosym: San Diego, CA, 1994.

(45) Dauber-Osguthorpe, P.; Roberts, V. A.; Osguthorpe, D. J.; Wolff, J.; Genest, M.; Hagler, A. T. *Proteins: Structure, Function and Genetics* **1988**, *4*, 31.

(46) *Computer Simulation of Solids;* Catlow, C. R. A., Ed.; Springer-Verlag: Berlin, 1982.

(47) *Modeling of Structure and Reactivity in Zeolites;* Catlow, C. R. A., Ed.; Academic Press: London, 1992.

(48) Deem, M. W.; Newsam, J. A.; Creighton, J. *J. Am. Chem. Soc.* **1992**, *114*, 7198.

(49) Smirnov, K. S.; Bougeard, D. *Zeolites* **1994**, *14*, 203.

(50) Jacobs, P. A. *Catal. Rev. Sci. Eng.* **1982**, *24*, 415.

(51) Derouane, E. G.; Fripiat, J. G. *J. Phys. Chem.* **1987**, *91*, 145.

(52) Rabo, J. A.; Gajda, G. *J. Catal. Rev. Sci. Eng.* **1990**, *31*, 385.

(53) Baekelandt, B.; De Tavernier, S.; Schoonheydt, R. A. Molecular Modeling of Petroleum Processes and Catalysis ACS San Francisco Meeting, 1992, p 506.

(54) Sauer, J. *Chem. Rev.* **1989**, *89*, 199.

(55) Verlet, L. *Phys. Rev.* **1967**, *159*, 98.

(56) Dempsey, E. *J. Phys. Chem.* **1969**, *73*, 3660.

(57) Terasaki, O.; Ymamazaki, K.; Thomas, J. M.; Ohsuna, T.; Watanabe, D.; Sanders, J. V.; Barry, J. C. *J. Solid State Chem.* **1988**, *77*, 72−83.

(58) Terasaki, O. *J. Electron Microsc.* **1994,** *43*, 337−346.

(59) Zandbergen, H. W.; van Dick, D. In *Proc. XIth Int. Congress on Electron Microscopy*, Kyoto, 1986.

(60) Zandbergen, H. W.; van Hoof, J. H. C. In *Proc. XIth Int. Congress on Electron Microscopy*, Kyoto, 1986.

(61) Bovin, J. O.; Alfredsson, V.; Blum, Z.; Karlsson, G.; Terasaki, O. In: *XIIIth Int. Congress on Electron Microscopy*, Paris, 1994.

(62) Rice, S. B.; Treacy, M. M. J.; Disko, M. M. In *XIIth Int. Congress on Electron Microscopy*, 1990.

(63) Terasaki, O.; Ohsuna, T. *Catal. Today* **1995**, *23*, 201−218.

(64) Hovmoller, S.; Sjogren, A.; Farrants, G.; Sundberg, M.; Marinder, B. O. *Nature* **1984**, *311*, 238−241.

(65) Hovmoller, S. *Ultramicroscopy* **1992**, *41*, 121−135.